ChemComm

Electrochemical and Microstructural Analysis of LiNi1/3Mn1/3Co1/3O2 Cathode Composites Prepared using SEED Method

Journal:	*ChemComm*
Manuscript ID	CC-COM-05-2024-002113.R1
Article Type:	Communication

Data availability statements

The data supporting this article have been included as part of the Supplementary Information. Crystallographic data for $LiNi_{1/3}Mn_{1/3}Co_{1/3}O_2$, $Li_{10}P_3S_{12}I$, Li_4PS_4I, Li_2S have been deposited at the ICSD under #184452, #54663, #123878, and #196932.

COMMUNICATION

Electrochemical and Microstructural Analysis of $LiNi_{1/3}Mn_{1/3}Co_{1/3}O_2$ Cathode Composites Prepared using SEED Method

Received 00th January 20xx,
Accepted 00th January 20xx

DOI: 10.1039/x0xx00000x

Kazuhiro Hikima [a,*], Yosuke Hamasaki [a], Masayo Takahashi [a], Reiko Matsuda [a], Hiroyuki Muto [a,b], and Atsunori Matsuda [a,*]

Cathode composites were fabricated using the nuclear growth (SEED) method, where Li_2S seeds on the active materials grow to solid electrolyte precursors in the corresponding Li_2S-P_2S_5-LiI solution. Compared to mortar mixing, the SEED method demonstrated higher cycle stability, with a $90LiNi_{1/3}Mn_{1/3}Co_{1/3}O_2$-$10Li_7P_2S_8I$ (Li_2S:P_2S_5:LiI = 3:1:1 (wt%)) composite retaining 99.7% discharge capacity after six cycles compared to 66.1% with mortar mixing. Cross-sectional scanning electron microscope-energy dispersive X-ray spectroscopy images suggest that the solid electrolyte was more uniformly distributed in the cathode composite prepared using the SEED method. This study opens up the potential for higher cathode-active material loading ratios and ASSBs with higher energy densities.

All-solid-state batteries (ASSBs), wherein the organic electrolyte used in lithium-ion batteries is replaced with a flame-retardant ceramic solid electrolyte, have garnered significant attention in recent years. Their operating principle is similar to that of conventional lithium-ion batteries, except that Li ions are transferred between solid-state active materials. Some notable advantages of ASSBs include the absence of flammable organic electrolytes and no risks of leakage or ignition. Additionally, the simplicity of the equipment and ease of lamination contribute to their high energy density and output power.[1-2] A previous study demonstrated that all-solid-state batteries offer higher energy density and power output compared to currently used organic liquid batteries and supercapacitors.[1] However, ASSBs exhibit the tendency of cracking and performance degradation owing to the stress of repeated charge–discharge cycles and the high grain boundary resistance between solid particles.

Sulphide and oxide electrolytes are the current front-runners for practical solid electrolytes. Sulphide-type electrolytes, such as $Li_{10}GeP_2S_{12}$, show high ionic conductivity (10^{-2} S cm^{-1}) and sufficient plasticity, which allow interface formation under pressure at room temperature.[3] However, they react with atmospheric moisture to produce H_2S gas, which is hazardous to humans.[4] Sulphide materials are divided into glasses (e.g., $70Li_2S$-$30P_2S_5$),[5] glass ceramics (e.g., $Li_7P_2S_8I$ and $Li_7P_3S_{11}$),[6-7] and crystals (e.g., $Li_{10}GeP_2S_{12}$ and Li_6PS_5Cl).[1, 3, 8] In addition, the interface between an oxide cathode material (e.g., $LiCoO_2$) and a sulphide solid electrolyte features an electrochemical potential difference, which changes the Li-ion concentration.[9] Introducing $LiNbO_3$ as a buffer layer at the oxide cathode and sulphide solid electrolyte interface can address this issue.[10] In contrast, oxide-type electrolytes possess candidate materials such as the garnet-type $Li_7La_3Zr_2O_{12}$ structure, which exhibits stability in the atmosphere and an ionic conductivity of approximately 10^{-3} S cm^{-1}; however, they require high sintering temperatures and present physical contact challenges.[11]

The electrode layer of an ASSB comprises electrode-active materials that store only Li ions. However, active electrode materials possess low electronic and ionic conductivities; thus, they face interface formation issues. Therefore, the electrode layer is generally composed of a solid electrolyte, which facilitates ion transport in the electrode layer, and a conductive aid, which ensures electron transport. To fabricate high-performance ASSBs, a composite structure that forms a solid interface within the electrode composite and provides effective electron and ion conduction pathways must be designed.[12] A solid electrolyte coating on an electrode-active material has been suggested to construct uniform ionic conduction pathways. This coating method prevents particle agglomeration within the electrode layer and enables the formation of ionic conduction pathways with a minimal amount of solid electrolyte. In addition, the previous reports show that the formation of an ionic conductor at the surface of the cathode material improves overall battery performance [13-15]. The coating methods may be broadly classified into vapour-, liquid-, and solid-phase methods. Pulsed laser deposition (PLD) is a vapour-phase method[16] that can be used to create uniform electrolyte films, provide high-precision film controllability, and be integrated into various interfacial configurations. However, it requires high-cost equipment and is unsuitable for mass production. For solid-phase methods, dry coating methods such

[a] *Department of Electrical and Electronic Information Engineering, Toyohashi University of Technology, 1-1 Hibarigaoka, Tempaku, Toyohashi, Aichi 441-8580, Japan.*
[b] *Institute of Liberal Arts and Sciences, Toyohashi University of Technology, 1-1 Hibarigaoka, Tempaku, Toyohashi, Aichi 441-8580, Japan*
E-mail: hikima.kazuhiro.ou@tut.jp, matsuda.atsunori.hh@tut.jp
† Footnotes relating to the title and/or authors should appear here.
Electronic Supplementary Information (ESI) available: [details of any supplementary information available should be included here]. See DOI: 10.1039/x0xx00000x

as mechano-fusion have been suggested.[17-18] However, similar to vapour-phase methods, they do not cater to industrial applications due to their high energy requirements and incompatibility with mass production. In the liquid-phase method, solid electrolytes synthesised using the solid-phase method are initially dissolved in an organic solvent and then coated onto the active material upon solvent removal.[19] Due to its scalability, the liquid-phase method features the highest practical feasibility for use as a coating technique.

In this study, cathode composites were fabricated using a nuclear growth (SEED) method developed in our laboratory.[20-22] In the SEED method, Li_2S are initially formed as seeds on the active materials, and then the solid electrolyte precursors are precipitated and grown from the nuclear seeds in the corresponding Li_2S-P_2S_5-LiI solution. Then, the $Li_7P_2S_8I$ solid electrolyte is coated homogeneously.[20-22] Compared with conventional methods such as mortar mixing, the SEED method, a liquid-phase coating technique, produces cathode composites with uniform ionic conduction pathways using a low solid electrolyte mass (10 wt%) for ASSBs. The SEED method in this study, which is an improved version, features the sonication step to enhance homogeneity, which has not been employed in previous studies.[20-21] In addition, to the best of the authors' knowledge, the electrochemical and microstructural analysis of cathode composites was conducted for the first time. These analyses indicated that the SEED method yields a unique microstructure and results in the formation of a percolation network within the cathode composite even at a low solid electrolyte ratio of 10 wt%. Fig. 1 presents the XRD patterns of $90LiNi_{1/3}Mn_{1/3}Co_{1/3}O_2$-$10Li_7P_2S_8I$ prepared using the SEED method, $100Li_7P_2S_8I$ without the cathode-active material (SEED), and $100Li_7P_2S_8I$ prepared using liquid-phase shaking and used for hand-mixing (LS). The only peaks belonging to $LiNi_{1/3}Mn_{1/3}Co_{1/3}O_2$(ICSD #184452) were observed for the $90LiNi_{1/3}Mn_{1/3}Co_{1/3}O_2$-$10Li_7P_2S_8I$ cathode composite. This may be attributed to the small ratio (10 wt%) of $Li_7P_2S_8I$ in the cathode composite and the low peak intensity of $Li_7P_2S_8I$ because $Li_7P_2S_8I$ is a glass ceramic.

In contrast, $Li_7P_2S_8I$ synthesised using the SEED method exhibited only the pattern of the Li_4PS_4I phase, which possessed a lower ionic conductivity of 1.0×10^{-4} S cm^{-1}.[23] The crystal structure of $Li_7P_2S_8I$ synthesised by the LS method is a composite of Li_4PS_4I, LiI, Li_2S and LGPS-type phases($Li_{10}P_3S_{12}I$), which exhibits a high ionic conductivity of 9.0×10^{-3} S cm^{-1}.[23],[24] The SEED method reduced the residual LiI in the starting materials compared with the LS method; however, a highly ionic LGPS conducting phase($Li_{10}P_3S_{12}I$) was not detected.

The Nyquist plots of $Li_7P_2S_8I$ synthesised using the LS and SEED methods at room temperature are shown in Fig. S4. The ionic conductivities of $Li_7P_2S_8I$ synthesised by the LS and SEED methods were 4.8×10^{-4} S cm^{-1} and 1.8×10^{-5} S cm^{-1}, respectively. The $Li_7P_2S_8I$ synthesised SEED method mainly shows the Li_4PS_4I phase and a highly ionic LGPS conducting phase was not detected, which was observed in the $Li_7P_2S_8I$ synthesised using the LS method. Thus, the difference in the crystalline phases results in a decrease in the ionic conductivity by approximately one order of magnitude. The difference in the crystal phases was determined through XRD pattern analyses. The LS sample shows the Li_4PS_4I phase and LiI, whose ionic conductivity is lower than that of the $Li_{10}P_3S_{12}I$ phase with an LGPS-type structure, and thus, the difference between the ionic conductivities of the samples synthesised by LS and SEED methods can be observed.

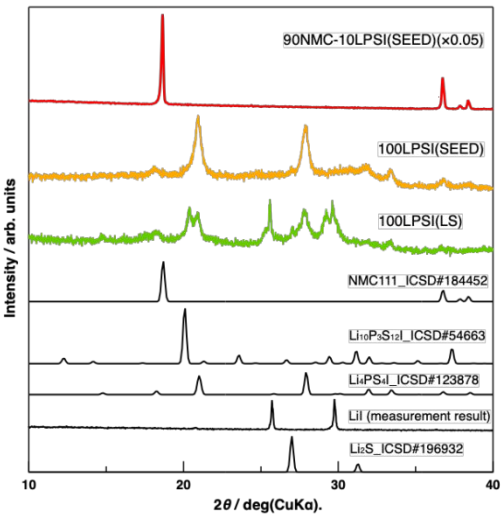

Fig. 1. X-ray diffraction (XRD) patterns of the $90NMC\text{-}10Li_7P_2S_8I$ prepared by the SEED method; $100Li_7P_2S_8I$, without cathode active material (SEED); and $100Li_7P_2S_8I$, used for hand mixing (LS).

Figs. 2a and 2b show the results of the DC polarisation tests of the cathode composites prepared using the hand-mixing and SEED methods, respectively. The electronic conductivities of the cathode composites were calculated based on these results. The electronic conductivities of the composites synthesised by hand-mixing and the SEED methods were 9.4×10^{-6} and 1.9×10^{-6} S cm^{-1}, respectively. The hand-mixing method yielded a slightly greater electronic conductivity, suggesting that coating the active material using the SEED method diminished the active material's contribution to electronic conductivity. Figs. 2c and 2d show the Nyquist plots of the cathode composites prepared by hand-mixing and the SEED method. The ionic conductivities calculated from the Nyquist plots were 5.1×10^{-5} and 3.7×10^{-5} S cm^{-1} for the hand-mixing and the SEED methods, respectively, which were similar. Surprisingly, there was a slight difference in ionic conductivity between the two synthesis methods, despite the lower ionic conductivity of $Li_7P_2S_8I$ synthesised using the SEED method. We conducted the SEM analysis to determine the reason for the slight difference in ionic conductivity between the two synthesis methods, despite the $Li_7P_2S_8I$ synthesised by the SEED method showing a lower ionic conductivity in the next section.

Fig. S3 shows the SEM images of the $LiNi_{1/3}Mn_{1/3}Co_{1/3}O_2$ and $90LiNi_{1/3}Mn_{1/3}Co_{1/3}O_2$-$10Li_7P_2S_8I$ cathode composites prepared using hand-mixing and the SEED method. The NMC comprised spheres with diameters of approximately 3 µm. The hand-mixed sample exhbited $Li_7P_2S_8I$ particles that were isolated from the $LiNi_{1/3}Mn_{1/3}Co_{1/3}O_2$ particles; the isolated particles did not contribute to the ionic conduction pathway and reduced energy density. However, a uniform coating was observed on the

surface of $LiNi_{1/3}Mn_{1/3}Co_{1/3}O_2$ created using the SEED method, indicating the potential for a consistent ionic conduction pathway between the active material and the solid electrolyte within the cathode composite. Fig. S4 shows the SEM-EDX images of the $90LiNi_{1/3}Mn_{1/3}Co_{1/3}O_2$-$10Li_7P_2S_8I$ cathode composite prepared by the SEED method. The EDX mapping image shows that S and P, derived from the $Li_7P_2S_8I$ solid electrolyte, are detected on the $LiNi_{1/3}Mn_{1/3}Co_{1/3}O_2$ particles. This result indicated that the $Li_7P_2S_8I$ solid electrolyte was formed at the surface of the $LiNi_{1/3}Mn_{1/3}Co_{1/3}O_2$ particle. In addition, the thickness of the $Li_7P_2S_8I$ solid electrolyte coated on the $LiNi_{1/3}Mn_{1/3}Co_{1/3}O_2$ particle was calculated. If the $LiNi_{1/3}Mn_{1/3}Co_{1/3}O_2$ particle is approximated as a 3-μm sphere, its surface area is 28.3 μm. Hence, the thickness of the $Li_7P_2S_8I$ can be approximately 100 nm for the $90LiNi_{1/3}Mn_{1/3}Co_{1/3}O_2$-$10Li_7P_2S_8I$ (wt%)(=82:18 vol%) cathode composite.

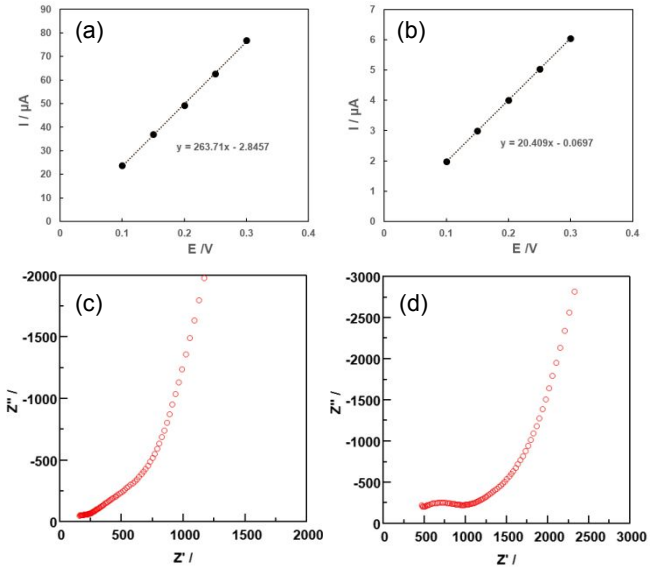

Fig. 2. DC polarisation test results for $90LiNi_{1/3}Mn_{1/3}Co_{1/3}O_2$-$10Li_7P_2S_8I$ cathode composite prepared by (a) hand-mixing (b) SEED method; Nyquist plots of $Li_{5.5}PS_{4.5}Cl_{1.5}$/$90LiNi_{1/3}Mn_{1/3}Co_{1/3}O_2$-$10Li_7P_2S_8I$ cathode composite prepared by (c) Hand-mixing (d) SEED method.

Fig. 3 illustrates the cross-sectional SEM-EDX mapping of the cathode composites prepared using hand-mixing and the SEED methods. The phosphorus (P) and sulphur (S) derived from the solid electrolyte clustered in the composite prepared by hand-mixing. This agglomeration may result in the loss of the ionic conduction pathway and a decrease in energy density owing to the non-uniform distribution between the active material and the solid electrolyte. In contrast, in the SEED cathode composite, phosphorus (P) and sulphur (S) are uniformly distributed. This uniform distribution of the solid electrolyte may be attributed to the coating of the active material in the precursor solution. As observed in the cross-sectional SEM images, the solid electrolyte was uniformly coated on the composite using the SEED method. By integrating this method, a percolation network is estimated to form within the cathode composite, even at a low solid electrolyte ratio of 10 wt%. These results explain the slight difference in ionic conductivity between the two synthesis methods, despite the lower ionic conductivity of $Li_7P_2S_8I$ synthesised by the SEED method. In addition, the SEED method in this study featured better homogeneity owing to the application of sonication.[21]

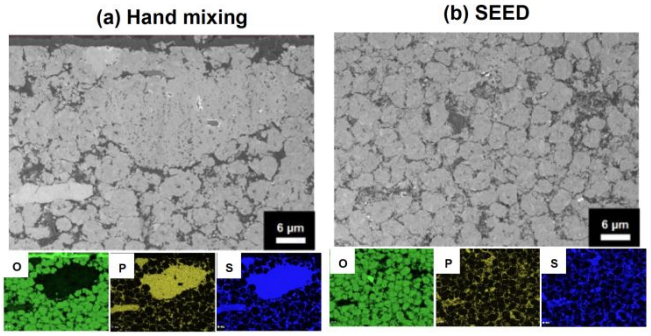

Fig. 3. Cross-sectional scanning electron microscopy with energy-dispersive X-ray spectroscopy (SEM-EDX) images of $90LiNi_{1/3}Mn_{1/3}Co_{1/3}O_2$-$10Li_7P_2S_8I$ (wt%) prepared by (a) hand-mixing and (b) SEED method.

Fig. 4 illustrates the charge–discharge curves of the cathode composites prepared using the hand-mixing and SEED methods. The initial discharge capacity for the cathode composite prepared using the SEED method was 103 mAh g^{-1}, which was slightly lower than that of the composite prepared using hand-mixing (110 mAh g^{-1}). This is due to the lower ionic and electronic conductivity of the cathode composite synthesized by the SEED method (Fig.2). However, it retained 99.7% of its discharge capacity after six cycles. In the cathode composite prepared using the SEED method, irreversible capacity was only observed in the first cycle. In contrast, with the hand-mixing method, irreversible capacity was consistently observed throughout cycling. These results indicated that the uniform synthesis of the solid electrolyte within the composite by the SEED method, particularly the direct coating on the surface of the active material, is believed to enable the solid electrolyte to accommodate the changes in the volume of the cathode active material during Li-ion (de-)intercalation. This relaxation of volume expansion and shrinkage prevents the formation of voids and cracks, inhibiting the separation of cathode-active material particles. In the cathode composite prepared via the hand-mixing method, cycling-induced volume changes lead to the formation of voids and cracks, gradually compromising the ionic conduction pathway. This phenomenon is closely associated with the observed irreversible capacity. In addition, the ASSB in this study showed a higher discharge capacity than that in the previous study.[21] This result indicates that the homogeneity of solid electrolytes was improved in this study, and the Li-ion from more cathode-active materials could be extracted.

Despite the relatively small volume change of $LiNi_{1/3}Mn_{1/3}Co_{1/3}O_2$ due to Li-ion (de-)intercalation (approximately 1%), it is in significant contrast with other active materials.[25] The advantages of the SEED method can be further enhanced by applying it to active materials that experience considerable volume change during operation, such as graphite and silicon. Thus, the composites fabricated using the SEED method showed promising results; however, the conductivity of the solid electrolyte in the SEED method under the present conditions was still low. Therefore, enhancing the conductivity is essential for achieving high-power characteristics in the future. Specifically, the solid electrolyte composition could be

improved and diversified, for example, $Li_{10}P_3S_{12}I$ and $Li_{10}P_3S_{12}Br$, which can be synthesized with heat treatment at lower temperatures.

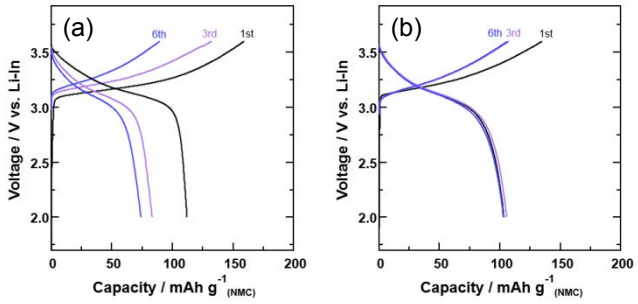

Fig. 4. Charge–discharge curves of the all-solid-state Li-ion battery using $90LiNi_{1/3}Mn_{1/3}Co_{1/3}O_2$-$10Li_7P_2S_8I$ prepared by (a) hand-mixing and (b) SEED method at 30 °C under cutoff voltage (2.0 to 3.6) V vs. Li-In.

In this study, cathode composites, which are expected to be useful in practical ASSBs, were prepared using the SEED method for coating sulphide solid electrolytes. This study aimed to establish uniform electron and ion conduction pathways within a cathode composite. To this end, a $90LiNi_{1/3}Mn_{1/3}Co_{1/3}O_2$-$10 Li_7P_2S_8I$ (wt%) cathode composite, which possesses a lower solid electrolyte ratio than the conventional ratio (for example, $70LiNi_{1/3}Mn_{1/3}Co_{1/3}O_2$-30 $Li_7P_2S_8I$(wt%)), was fabricated using the SEED method as the improved version. The cross-sectional SEM-EDX images revealed that $Li_7P_2S_8I$ was formed on the surface of $LiNi_{1/3}Mn_{1/3}Co_{1/3}O_2$ within the cathode composite for the first time. The charge–discharge curves showed the stable cycle performance of the cathode composite, despite the high ratio of active material. This stability may be attributed to the uniform coating due to the higher homogeneity of solid electrolytes in this study, which can absorb the volume change of the active materials and prevent the loss of ionic conduction pathways. While the cathode composites fabricated using the SEED method, as the improved version, showed similar ionic conductivity to that fabricated through hand-mixing, the conductivity of the solid electrolyte in the SEED method was still low under the present conditions. Therefore, enhancing conductivity is essential for achieving high-power characteristics in future work. This work was supported by JSPS KAKENHI (Grant Numbers JP 21K14716 and 22H04614); the GteX Program (JPMJGX23S5) of the Japan Science and Technology Agency (JST), Japan; and the Mazda Foundation.

Author Contributions

Conceptualisation, K.H., R.M., and A.M.; methodology, Y.H., M.T.; software, Y.H., M.T.; validation, K.H., Y.H.; formal analysis, K.H., Y.H., M.T.; investigation, K.H., Y.H.; resources, K.H., H.M., A.M.; data curation, K.H., Y.M.; writing — original draft preparation, K.H.; writing — review and editing, K.H., Y.M., R.M., and A.M.; visualisation, K.H., Y.H.; supervision, K.H., H.M., A.M.; project administration, K.H., H.M., A.M.; funding acquisition, K.H., H.M., A.M.; All authors have read and agreed to the published version of the manuscript.

Conflicts of interest

There are no conflicts to declare.

References

[1] Y. Kato; S. Hori; T. Saito; K. Suzuki; M. Hirayama; A. Mitsui; M. Yonemura; H. Iba; R. Kanno, *Nature Energy,* 1 (2016) 16030.
[2] J. Schnell; F. Tietz; C. Singer; A. Hofer; N. Billot; G. Reinhart, *Energy & Environmental Science,* 12 (2019) 1818-1833.
[3] N. Kamaya; K. Homma; Y. Yamakawa; M. Hirayama; R. Kanno; M. Yonemura; T. Kamiyama; Y. Kato; S. Hama; K. Kawamoto; A. Mitsui, *Nature Materials,* 10 (2011) 682.
[4] A. Sakuda; A. Hayashi; M. Tatsumisago, *Sci Rep,* 3 (2013) 2261.
[5] F. Mizuno; A. Hayashi; K. Tadanaga; M. Tatsumisago, *Advanced Materials,* 17 (2005) 918-921.
[6] E. Rangasamy; Z. Liu; M. Gobet; K. Pilar; G. Sahu; W. Zhou; H. Wu; S. Greenbaum; C. Liang, *Journal of the American Chemical Society,* 137 (2015) 1384-1387.
[7] A. Hayashi; K. Minami; S. Ujiie; M. Tatsumisago, *Journal of Non-Crystalline Solids,* 356 (2010) 2670-2673.
[8] Y. Li; S. Song; H. Kim; K. Nomoto; H. Kim; X. Sun; S. Hori; K. Suzuki; N. Matsui; M. Hirayama; T. Mizoguchi; T. Saito; T. Kamiyama; R. Kanno, *Science,* 381 (2023) 50-53.
[9] M. Haruta; S. Shiraki; T. Suzuki; A. Kumatani; T. Ohsawa; Y. Takagi; R. Shimizu; T. Hitosugi, *Nano Lett,* 15 (2015) 1498-502.
[10] N. Ohta; K. Takada; I. Sakaguchi; L. Zhang; R. Ma; K. Fukuda; M. Osada; T. Sasaki, *Electrochemistry Communications,* 9 (2007) 1486-1490.
[11] R. Murugan; V. Thangadurai; W. Weppner, *Angewandte Chemie International Edition,* 46 (2007) 7778-7781.
[12] S. Noh; W. T. Nichols; M. Cho; D. Shin, *Journal of Electroceramics,* 40 (2018) 293-299.
[13] Y.-J. Yen; S.-H. Chung, *ACS Applied Materials & Interfaces,* 13 (2021) 58712-58722.
[14] C. Wang; K. Aoyagi; P. Wisesa; T. Mueller, *Chemistry of Materials,* 32 (2020) 3741-3752.
[15] Y.-J. Yen; S.-H. Chung, *Journal of Materials Chemistry A,* 11 (2023) 4519-4526.
[16] A. Sakuda; A. Hayashi; T. Ohtomo; S. Hama; M. Tatsumisago, *Journal of Power Sources,* 196 (2011) 6735-6741.
[17] J. Kim; M. J. Kim; J. Kim; J. W. Lee; J. Park; S. E. Wang; S. Lee; Y. C. Kang; U. Paik; D. S. Jung; T. Song, *Advanced Functional Materials,* 33 (2023).
[18] E. Hayakawa; H. Nakamura; S. Ohsaki; S. Watano, *Advanced Powder Technology,* 33 (2022).
[19] S. Yubuchi; S. Teragawa; K. Aso; K. Tadanaga; A. Hayashi; M. Tatsumisago, *Journal of Power Sources,* 293 (2015) 941-945.
[20] R. Matsuda; E. Hirahara; N. H. H. Phuc; H. Muto; H. Tsukasaki; S. Mori; A. Matsuda, *Journal of the Ceramic Society of Japan,* 126 (2018) 826-831.
[21] R. Matsuda; E. Hirabara; N. H. H. Phuc; H. Muto; A. Matsuda, *IOP Conference Series: Materials Science and Engineering,* 429 (2018).
[22] M. Calpa; N. C. Rosero-Navarro; A. Miura; K. Tadanaga; A. Matsuda, *Solid State Ionics,* 372 (2021).
[23] S. J. Sedlmaier; S. Indris; C. Dietrich; M. Yavuz; C. Dräger; F. von Seggern; H. Sommer; J. Janek, *Chemistry of Materials,* 29 (2017) 1830-1835.
[24] S. Song; S. Hori; Y. Li; K. Suzuki; N. Matsui; M. Hirayama; T. Saito; T. Kamiyama; R. Kanno, *Chemistry of Materials,* 34 (2022) 8237-8247.
[25] S. C. Yin; Y. H. Rho; I. Swainson; L. F. Nazar, *Chemistry of Materials,* 18 (2006) 1901-1910.